Parallel generation of 31 tripartite entangled states based on optical frequency combs*

Jing Zhang(张静)[1,2,3,†], Yan-Fang Wang(王艳芳)[1,2], Xiao-Yu Liu(刘晓宇)[1,2], and Rong-Guo Yang(杨荣国)[1,2,3]

[1] *State Key Laboratory of Quantum Optics and Quantum Optics Devices, Shanxi University, Taiyuan* 030006, *China*
[2] *College of Physics and Electronic Engineering, Shanxi University, Taiyuan* 030006, *China*
[3] *Collaborative Innovation Center of Extreme Optics, Shanxi University, Taiyuan* 030006, *China*

(Received 5 June 2017; revised manuscript received 3 August 2017; published online 20 October 2017)

Quantum entangled states, especially those having particular properties, are key resources for quantum information and quantum computation. In this paper, we put forward a new scheme to produce 31 continuous–variable (CV) tripartite entanglement fields based on three optical frequency combs via cascade nonlinear processes in an optical parametric cavity, and investigate the spectral characteristics of three frequency combs. The center wavelengths of the three combs are designed as 852 nm, 780 nm (atomic transition lines), and 1550 nm (fiber communication wavelength). The positivity under partial transposition (PPT) criterion, which is sufficient and necessary, is used to evaluate the entanglement in each group of comb lines. This scheme is experimentally feasible and valuable for constructing quantum information networks in future.

Keywords: quantum optics, nonlinear optics, quantum fluctuation

PACS: 42.50.–p, 42.65.–k, 42.50.Lc **DOI:** 10.1088/1674-1056/26/12/124205

1. Introduction

Quantum entanglement has been extensively applied in quantum information fields, such as quantum teleportation,[1] quantum dense coding,[2] and quantum key distribution,[3] etc. Diverse quantum entangled states have been studied intensively both theoretically and experimentally.[4–6] Generally, the continuous–variable (CV) bipartite entanglement can be generated in diverse systems, such as optical parametric amplifier (OPA) or optical parametric oscillator (OPO),[7,8] combination of two squeezed lights with a beam splitter,[9,10] and can be applied in different protocols of quantum communication.[11,12] In recent years, generating CV multipartite entangled states has been widely investigated in diverse methods, such as cascaded nonlinear processes,[13,14] dual-ported frequency doubling process,[15,16] and four-wave mixing process.[17–21] On the one hand, multipartite entangled states with different frequencies, especially including the fiber communication windows and the atomic transition lines, are more practical in applications of quantum communication networks and quantum storage. Such kind of three-color entanglement has been demonstrated both theoretically and experimentally in two cascaded NOPOs in 2012.[14,22]

On the other hand, quantum entanglement resources with high efficiency and multi-channel for quantum communication network is becoming a popular branch in quantum optics. The optical frequency comb is one of the ideal systems that can realize multi-channel and wavelength division multiplexing (WDM) for quantum communication network. In 2011, 15 quadripartite entangled cluster states were generated simultaneously in experiment via optical frequency combs.[23] A theoretical scheme to produce a multiplexed entanglement frequency comb in a nondegenerate optical parametric amplifier (NOPA) was proposed in 2013[24] and a low-frequency signal beyond the quantum limit was obtained via frequency-shift detection using frequency combs in 2015.[25] In addition, a large-scale cluster entangled state, which is necessary for usable quantum computation and quantum information processes, can also be generated by using an optical frequency comb. A cluster entangled state with more than 60 modes of a quantum optical frequency comb was achieved experimentally in 2014.[26] A theoretical scheme to produce CV cluster-state over the optical spatial mode was proposed in 2014.[27] The scheme of 11 entangled high-order transverse modes generated from an optical spatial mode comb was proposed recently.[28] The related research about the optical frequency comb have aroused many interests in theory and experiment. In this paper, we put forward a new scheme to produce 31 CV tripartite entanglement fields based on three optical frequency combs via parametric down-conversion (PDC) and sum-frequency generation (SFG) processes with a $\chi^{(2)}$ crystal in an OPO, which pumped by two fields (1573 nm and 550 nm). The center wavelengths of three combs are designed as 852 nm, 780 nm (transition line of Cs and Rb atoms) and 1550nm (optical fiber communication wavelength), for practi-

*Project supported by the National Natural Science Foundation of China (Grant Nos. 11504218, 11634008, 11674203, 11574187, 61108003, and 61227902), and the National Key Research and Development Program of China (Grant No. 2016YFA0301404).

†Corresponding author. E-mail: zjj@sxu.edu.cn

cal CV quantum information network with both storage nodes and fiber transmission lines.

The arrangements of detail are outlined as follows: In section 2, the theoretical model of frequency combs for 31 tripartite entangled states are introduced concisely and the evolution equations and the quadrature fluctuations of the three modes are deduced. Then the amplitude and phase quadrature of the three out-modes are calculated by employing the boundary conditions of optical cavities and the spectral characteristics of three frequency combs are investigated. In section 3, the PPT criterion is used to estimate the entanglement among each group of comb lines. Finally, a brief summary is presented in section 4.

2. Theoretical model and equations derivation

2.1. Theoretical model

The schematic of the system is shown in Fig. 1(a). The system consists of a dual-port OPO with three intra-cavity modes $(\hat{a}_1,\hat{a}_3,\hat{a}_5)$, two pump modes $(\hat{a}_2,\hat{a}_4)$, and a $\chi^{(2)}$ nonlinear crystal (the medium for PDC and SFG processes). Pump mode $\hat{a}_4$ is incident upon the optical medium to create modes $\hat{a}_1$ and $\hat{a}_3$ via PDC process, and synchronously the other pump mode $\hat{a}_2$ interacts with mode $\hat{a}_3$ to produce mode $\hat{a}_5$ via SFG process. The polarizations of all interacting modes are decided by the phase-matching conditions of the nonlinear crystal, which can be designed by a general method of photonic quasicrystals.[29] The energy conservation conditions are $\omega_4=\omega_1+\omega_3, \omega_5=\omega_2+\omega_3$. The quantum graph states of tripartite entanglement frequency comb is shown in Fig. 1(b). The center wavelengths of three optical frequency combs are designed as 852 nm, 1550 nm, and 780 nm (corresponding to $\omega_1,\omega_3,\omega_5$). The spectrums of three combs are separated in

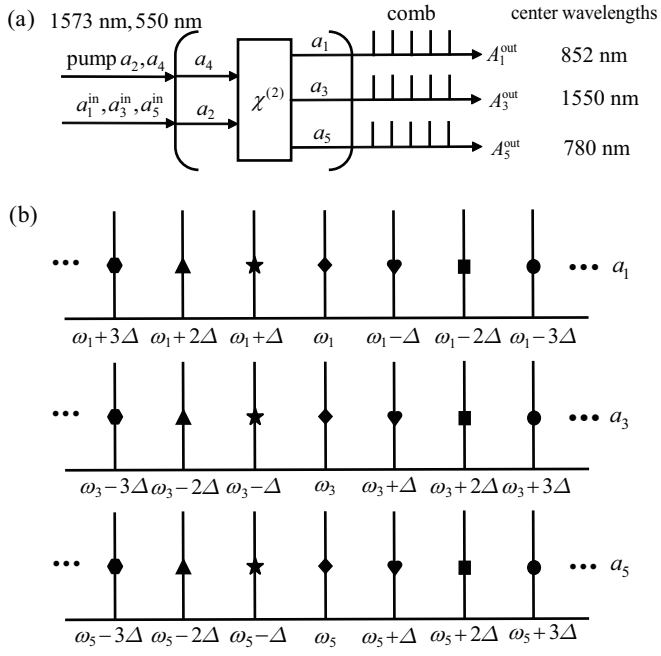

Fig. 1. (a) The schematic of the system for generation of tripartite entanglement frequency combs. (b) Quantum graph states of three out-modes, the comb lines scaled by the same symbol stands for a set of tripartite entanglement.

frequency by the cavity free spectral range (FSR) and are limited in bandwidth of nonlinear phase-matching. Each group of comb lines $\omega_1\pm n\Delta, \omega_3\mp n\Delta, \omega_5\mp n\Delta$ $(n=0,1,\ldots,15)$ scaled by the same symbol, represent a set of tripartite entanglement, where Δ is the FSR.

2.2. Equations derivation

The interaction Hamiltonian for the system is

$$\hat{H}_I = \mathrm{i}\hbar\chi^{(2)}(\hat{a}_4\hat{a}_1^\dagger\hat{a}_3^\dagger+\hat{a}_2\hat{a}_3\hat{a}_5^\dagger)+\mathrm{H.C.} \tag{1}$$

Under the condition of perfect phase matching without any detuning, the quantum Langevin equations of motion for the three modes can be expressed as

$$\begin{aligned}
\dot{\hat{a}}_1(t) &= -\gamma_1\hat{a}_1(t)+\chi^{(2)}\hat{a}_4(t)\hat{a}_3^\dagger(t)\\
&\quad+\sqrt{2\gamma_{b_1}}\hat{a}_1^{\mathrm{in}}(t)+\sqrt{2\gamma_{c_1}}\hat{c}_1(t),\\
\dot{\hat{a}}_3(t) &= -\gamma_1\hat{a}_3(t)+\chi^{(2)}\hat{a}_4(t)\hat{a}_1^\dagger(t)-\chi^{(2)}\hat{a}_2^\dagger(t)\hat{a}_5(t)\\
&\quad+\sqrt{2\gamma_{b_1}}\hat{a}_3^{\mathrm{in}}(t)+\sqrt{2\gamma_{c_1}}\hat{c}_3(t),\\
\dot{\hat{a}}_5(t) &= -\gamma_5\hat{a}_5(t)+\chi^{(2)}\hat{a}_2(t)\hat{a}_3(t)\\
&\quad+\sqrt{2\gamma_{b_5}}\hat{a}_5^{\mathrm{in}}(t)+\sqrt{2\gamma_{c_5}}\hat{c}_5(t),
\end{aligned} \tag{2}$$

where $\hat{a}_i$ $(i=1,3,5)$ is the annihilation operators of three intra-cavity modes. $\chi^{(2)}$ is the effective nonlinear coupling parameter and can be merged into pump field amplitude α_2 and α_4 (considered as χ_1 and χ_2, respectively). $\hat{a}_i^{\mathrm{in}}$ denotes the annihilation operators of the input modes. $\hat{c}_i$ $(i=1,3,5)$ is the vacuum noise term corresponding to intra-cavity loss. The total loss rate for each mode is $\gamma_i=\gamma_{b_i}+\gamma_{c_i}$, where γ_{b_i} corresponding to the loss rate of input and output coupler, and γ_{c_i} represents extra intra-cavity loss, which relates to absorption and surface scattering of crystal, imperfection of cavity mirrors, and so on. Here the loss of modes $\hat{a}_1$ and $\hat{a}_3$ are assumed to be equal.

The operator equations of cavity mode $\hat{a}_i$ $(i=1,3,5)$ after a single cavity round trip can be expressed as

$$\begin{aligned}
\hat{a}_1(t+\tau) &= \chi_1\tau\hat{a}_3^\dagger(t)+(1-\gamma_1\tau)\hat{a}_1(t)\\
&\quad+\sqrt{2\gamma_{b_1}}\tau\hat{a}_1^{\mathrm{in}}(t)+\sqrt{2\gamma_{c_1}}\tau\hat{c}_1(t),\\
\hat{a}_3(t+\tau) &= \chi_1\tau\hat{a}_1^\dagger(t)-\chi_2\tau\hat{a}_5(t)+(1-\gamma_1\tau)\hat{a}_3(t)\\
&\quad+\sqrt{2\gamma_{b_1}}\tau\hat{a}_3^{\mathrm{in}}(t)+\sqrt{2\gamma_{c_1}}\tau\hat{c}_3(t),\\
\hat{a}_5(t+\tau) &= \chi_2\tau\hat{a}_3(t)+(1-\gamma_5\tau)\hat{a}_5(t)\\
&\quad+\sqrt{2\gamma_{b_5}}\tau\hat{a}_5^{\mathrm{in}}(t)+\sqrt{2\gamma_{c_5}}\hat{c}_5(t),
\end{aligned} \tag{3}$$

where τ is the round-trip time of light in the cavity and it is assumed to be the same value for the three modes. It is convenient to decompose the field operators into the mean value and quantum fluctuations in the form $\hat{a}_i=\alpha_i+\delta\hat{a}_i$. After taking Fourier transforms of Eqs. (3), $\delta\hat{a}(t+\tau)\rightarrow$

$\delta\hat{a}(\omega)e^{i\omega\tau}, \delta\hat{a}(t) \to \delta\hat{a}(\omega)$, we can obtain the following equations in frequency domain

$$\begin{aligned}
&\delta\hat{a}_1(\omega)[e^{i\omega\tau}-(1-\gamma_1\tau)]\\
&= \chi_1\tau\delta\hat{a}_3^{\dagger}(\omega)+\sqrt{2\gamma_{b_1}}\tau\delta\hat{a}_1^{\rm in}(\omega)+\sqrt{2\gamma_{c_1}}\tau\delta\hat{c}_1(\omega),\\
&\delta\hat{a}_3(\omega)[e^{i\omega\tau}-(1-\gamma_1\tau)]\\
&= \chi_1\tau\delta\hat{a}_1^{\dagger}(\omega)-\chi_2\tau\delta\hat{a}_5(\omega)+\sqrt{2\gamma_{b_1}}\tau\delta\hat{a}_3^{\rm in}(\omega)\\
&\quad+\sqrt{2\gamma_{c_1}}\tau\delta\hat{c}_3(\omega),\\
&\delta\hat{a}_5(\omega)[e^{i\omega\tau}-(1-\gamma_5\tau)]\\
&= \chi_2\tau\delta\hat{a}_3(\omega)+\sqrt{2\gamma_{b_5}}\tau\delta\hat{a}_5^{\rm in}(\omega)+\sqrt{2\gamma_{c_5}}\tau\delta\hat{c}_5(\omega). \quad (4)
\end{aligned}$$

After complex calculating, the fluctuations of intra-cavity fields can be given as

$$\begin{aligned}
\delta\hat{a}_1(\omega) =& \frac{\{[e^{i\omega\tau}-(1-\gamma_1\tau)][e^{i\omega\tau}-(1-\gamma_5\tau)]+(\chi_2\tau)^2\}}{M}\\
&\times[\sqrt{2\gamma_{b_1}}\tau\delta\hat{a}_1^{\rm in}(\omega)+\sqrt{2\gamma_{c_1}}\tau\delta\hat{c}_1(\omega)]\\
&+\frac{\chi_1\tau[e^{i\omega\tau}-(1-\gamma_5\tau)]}{M}\\
&\times[\sqrt{2\gamma_{b_1}}\tau\delta\hat{a}_3^{\rm in\dagger}(\omega)+\sqrt{2\gamma_{c_1}}\tau\delta\hat{c}_3^{\dagger}(\omega)]\\
&-\frac{\chi_1\chi_2\tau^2}{M}[\sqrt{2\gamma_{b_5}}\tau\delta\hat{a}_5^{\rm in\dagger}(\omega)+\sqrt{2\gamma_{c_5}}\tau\delta\hat{c}_5^{\dagger}(\omega)],\\
\delta\hat{a}_3(\omega) =& \frac{\chi_1\tau[e^{i\omega\tau}-(1-\gamma_5\tau)]}{M}\\
&\times[\sqrt{2\gamma_{b_1}}\tau\delta\hat{a}_1^{\rm in\dagger}(\omega)+\sqrt{2\gamma_{c_1}}\tau\delta\hat{c}_1^{\dagger}(\omega)]\\
&+\frac{[e^{i\omega\tau}-(1-\gamma_1\tau)][e^{i\omega\tau}-(1-\gamma_5\tau)]}{M}\\
&\times[\sqrt{2\gamma_{b_1}}\tau\delta\hat{a}_3^{\rm in}(\omega)+\sqrt{2\gamma_{c_1}}\tau\delta\hat{c}_3(\omega)]\\
&-\frac{\chi_2\tau[e^{i\omega\tau}-(1-\gamma_1\tau)]}{M}\\
&\times[\sqrt{2\gamma_{b_5}}\tau\delta\hat{a}_5^{\rm in}(\omega)+\sqrt{2\gamma_{c_5}}\tau\delta\hat{c}_5(\omega)],\\
\delta\hat{a}_5(\omega) =& \frac{\chi_1\chi_2\tau^2}{M}[\sqrt{2\gamma_{b_1}}\tau\delta\hat{a}_1^{\rm in\dagger}(\omega)+\sqrt{2\gamma_{c_1}}\tau\delta\hat{c}_1^{\dagger}(\omega)]\\
&+\frac{\chi_2\tau[e^{i\omega\tau}-(1-\gamma_1\tau)]}{M}\\
&\times[\sqrt{2\gamma_{b_1}}\tau\delta\hat{a}+\sqrt{2\gamma_{c_1}}\tau\delta\hat{c}_3(\omega)]\\
&+\frac{\{[e^{i\omega\tau}-(1-\gamma_1\tau)]^2-(\chi_1\tau)^2\}}{M}\\
&\times[\sqrt{2\gamma_{b_5}}\tau\delta\hat{a}_5^{\rm in}(\omega)+\sqrt{2\gamma_{c_5}}\tau\delta\hat{c}_5(\omega)]. \quad (5)
\end{aligned}$$

The fluctuations of the output fields $\delta A_i^{\rm out}$ $(i=1,3,5)$ can be obtained by using the boundary condition $\delta\hat{A}_i^{\rm out}(\omega)=\sqrt{2\gamma_{b_i}}\delta\hat{a}_i(\omega)-\delta\hat{a}_i^{\rm in}(\omega)$. The amplitude and phase quadrature variances $(V_i^{\rm out\pm})$ of the three modes are

$$\begin{aligned}
V_1^{\rm out\pm}(\omega) =& \left|\frac{[e^{i\omega\tau}-(1-\gamma_1\tau)][e^{i\omega\tau}-(1-\gamma_5\tau)][2\gamma_{b_1}\tau-\gamma_1\tau+1-e^{i\omega\tau}]-(\chi_2\tau)^2[2\gamma_{b_1}\tau-\gamma_1\tau+1-e^{i\omega\tau}]+(\chi_1\tau)^2[e^{i\omega\tau}-(1-\gamma_5\tau)]}{M}\right|^2 V_1^{\rm in\pm}(\omega)\\
&+\left|\frac{2\sqrt{\gamma_{b_1}\gamma_{c_1}}\tau\{[e^{i\omega\tau}-(1-\gamma_1\tau)][e^{i\omega\tau}-(1-\gamma_5\tau)]+(\chi_2\tau)^2\}}{M}\right|^2 V_1^{c\pm}(\omega)+\left|\frac{2\gamma_{b_1}\chi_1\tau^2[e^{i\omega\tau}-(1-\gamma_5\tau)]}{M}\right|^2 V_3^{\rm in\pm}\\
&+\left|\frac{2\sqrt{\gamma_{b_1}\gamma_{c_1}}\chi_1\tau^2[e^{i\omega\tau}-(1-\gamma_1\tau)]}{M}\right|^2 V_3^{c\pm}(\omega)+\left|\frac{2\chi_1\chi_2\sqrt{\gamma_{b_1}\gamma_{b_5}}\tau^3}{M}\right|^2 V_5^{\rm in\pm}(\omega)+\left|\frac{2\chi_1\chi_2\sqrt{\gamma_{b_1}\gamma_{c_5}}\tau^3}{M}\right|^2 V_5^{c\pm}(\omega),\\
V_3^{\rm out\pm}(\omega) =& \left|\frac{[e^{i\omega\tau}-(1-\gamma_1\tau)][e^{i\omega\tau}-(1-\gamma_5\tau)][2\gamma_{b_1}\tau-\gamma_1\tau+1-e^{i\omega\tau}](\chi_2\tau)^2[e^{i\omega\tau}-(1-\gamma_1\tau)]+(\chi_1\tau)^2[e^{i\omega\tau}-(1-\gamma_5\tau)]}{M}\right|^2 V_3^{\rm in\pm}(\omega)\\
&+\left|\frac{2\sqrt{\gamma_{b_1}\gamma_{c_1}}\tau[e^{i\omega\tau}-(1-\gamma_1\tau)][e^{i\omega\tau}-(1-\gamma_5\tau)]}{M}\right|^2 V_3^{c\pm}(\omega)+\left|\frac{2\sqrt{\gamma_{b_1}\gamma_{b_5}}\chi_2\tau^2[e^{i\omega\tau}-(1-\gamma_1\tau)]}{M}\right|^2 V_5^{\rm in\pm}(\omega)\\
&+\left|\frac{2\gamma_{b_1}\chi_1\tau^2[e^{i\omega\tau}-(1-\gamma_5\tau)]}{M}\right|^2 V_1^{\rm in\pm}(\omega)+\left|\frac{2\sqrt{\gamma_{b_1}\gamma_{c_1}}\chi_1\tau^2[e^{i\omega\tau}-(1-\gamma_5\tau)]}{M}\right|^2 V_1^{c\pm}(\omega)\\
&+\left|\frac{2\sqrt{\gamma_{b_1}\gamma_{c_5}}\chi_2\tau^2[e^{i\omega\tau}-(1-\gamma_1\tau)]}{M}\right|^2 V_5^{c\pm}(\omega),\\
V_5^{\rm out\pm}(\omega) =& \left|\frac{2\sqrt{\gamma_{b_1}\gamma_{b_5}}\chi_1\chi_2\tau^3}{M}\right|^2 V_1^{\rm in\pm}(\omega)+\left|\frac{2\sqrt{\gamma_{b_5}\gamma_{c_1}}\chi_1\chi_2\tau^3}{M}\right|^2 V_1^{c\pm}(\omega)+\left|\frac{\sqrt{2\gamma_{b_1}\gamma_{b_5}}\chi_2\tau^2[e^{i\omega\tau}-(1-\gamma_1\tau)]}{M}\right|^2 V_3^{\rm in\pm}(\omega)\\
&+\left|\frac{\sqrt{2\gamma_{b_5}\gamma_{c_1}}\chi_2\tau^2[e^{i\omega\tau}-(1-\gamma_1\tau)]}{M}\right|^2 V_3^{c\pm}(\omega)+\left|\frac{2\sqrt{\gamma_{b_5}\gamma_{c_5}}\tau\{[e^{i\omega\tau}-(1-\gamma_1\tau)]^2-(\chi_1\tau)^2\}}{M}\right|^2 V_5^{c\pm}(\omega).\\
&+\left|\frac{[e^{i\omega\tau}-(1-\gamma_1\tau)]^2[2\gamma_{b_5}\tau-\gamma_5\tau+1-e^{i\omega\tau}]+(\chi_1\tau)^2[e^{i\omega\tau}-1+\gamma_5\tau-2\gamma_{b_5}\tau]-(\chi_2\tau)^2[e^{i\omega\tau}-(1-\gamma_1\tau)]}{M}\right|^2 V_5^{\rm in\pm}(\omega), \quad (6)
\end{aligned}$$

where $M = [e^{i\omega\tau}-(1-\gamma_1\tau)]^2[e^{i\omega\tau}-(1-\gamma_5\tau)]+(\chi_2\tau)^2[e^{i\omega\tau}-(1-\gamma_1\tau)]-(\chi_1\tau)^2[e^{i\omega\tau}-(1-\gamma_5\tau)]$.

The definitions of the amplitude and phase quadrature fluctuations of output modes, input modes and vacuum noise are

$$\begin{aligned}
\delta\hat{X}_i^{+}(\omega) &= [\delta\hat{A}_i^{\rm out}(\omega)+\delta\hat{A}_i^{\rm out}(-\omega)^{\dagger}],\\
\delta\hat{X}_i^{-}(\omega) &= i[\delta\hat{A}_i^{\rm out}(-\omega)^{\dagger}-\delta\hat{A}_i^{\rm out}(\omega)],\\
\delta\hat{X}_i^{\rm in+}(\omega) &= [\delta\hat{a}_i^{\rm in}(\omega)+\delta\hat{a}_i^{\rm in}(-\omega)^{\dagger}],
\end{aligned}$$

$$\begin{aligned}\delta\hat{X}_i^{\text{in}-}(\omega) &= \mathrm{i}[\delta\hat{a}_i^{\text{in}}(-\omega)^\dagger - \delta\hat{a}_i^{\text{in}}(\omega)],\\ \delta\hat{X}_i^{c+}(\omega) &= [\delta\hat{c}_i(\omega) + \delta\hat{c}_i(-\omega)^\dagger],\\ \delta\hat{X}_i^{c-}(\omega) &= i[\delta\hat{c}_i(-\omega)^\dagger - \delta\hat{c}_i(\omega)].\end{aligned} \tag{7}$$

The quadrature variances are defined by the following expressions: $V_i^{\text{out}\pm}(\omega) = \langle|\delta\hat{X}_i^{\pm}|^2\rangle$, $V_i^{\text{in}\pm}(\omega) = \langle|\delta\hat{X}_i^{\text{in}\pm}|^2\rangle$, $V_i^{c\pm}(\omega) = \langle|\delta\hat{X}_i^{c\pm}|^2\rangle$.

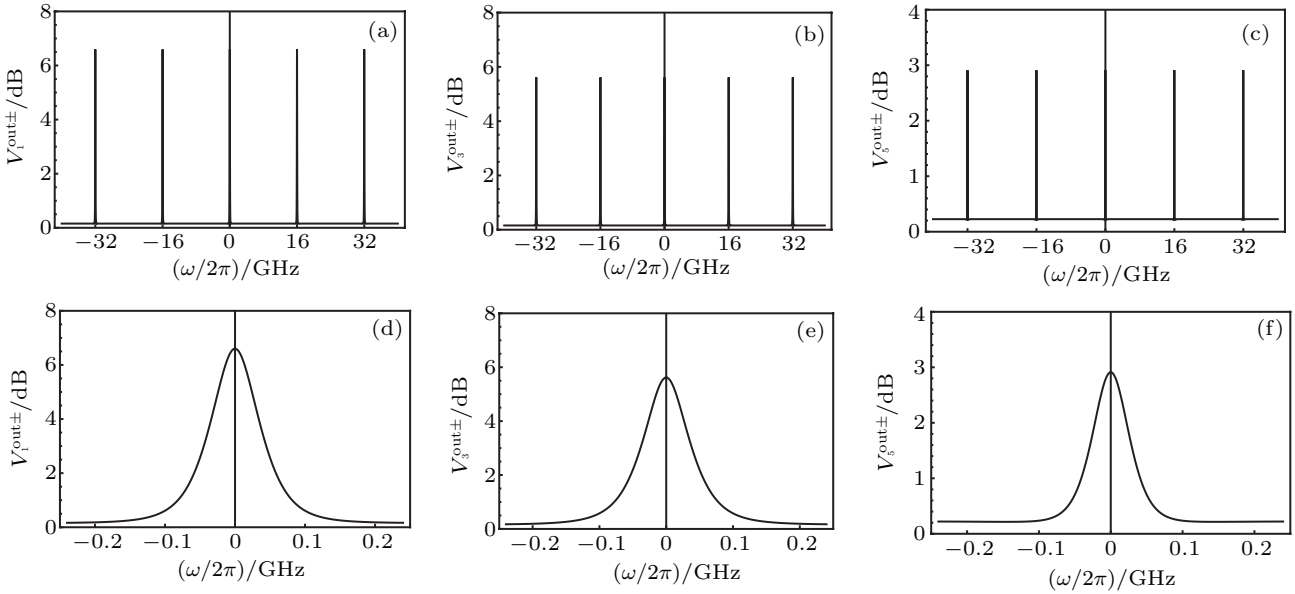

Fig. 2. The amplitude and phase quadrature variances versus analysis frequency for three modes. Panels (a), (b), (c) are corresponding to the quadrature variances of modes $\hat{a}_1$, $\hat{a}_3$, $\hat{a}_5$, respectively, and panels (d), (e), (f) show the details of the zero-order comb line.

Here we consider that $V_i^{\text{in}\pm}(\omega) = 1$, $V_i^{c\pm}(\omega) = 1$ $(i = 1,3,5)$, and the FSR is $16/2\pi$ GHz (optical circular frequency for calculation convenience). The amplitude and phase quadrature noise spectra of three modes versus the analysis frequency are given in Fig. 2. It is obvious that the frequency combs of three modes are equidistant lines in frequency space, and the amplitude and phase quadrature variances are all above the shot noise level for three modes. The line shapes of the zero-order and other ±n-order $(n = 1,2,\ldots 15)$ are the same.

Actually, the whole bandwidth of the comb is confined by the phase-matching bandwidth of the crystal. The optical cavity can increase nonlinear coupling and lead to spectral filtering of the down-converted and sum-frequency output. For a bulk nonlinear optical crystal of length L_{crystal}, the phase-matching bandwidth is approximately $10c/L_{\text{crystal}}$. The FSR of a cavity with length L_{cavity} is $c/2L_{\text{cavity}}$.[24,30] If we consider that $L_{\text{cavity}} = 5.88$ cm, $L_{\text{crystal}} = 1.96$ cm, which are experimental feasible parameters, then 31 tripartite entangled states can be excited.

3. Entanglement characteristics

For Gaussian states, the complete information is available from the mean values (first-order moments) and the covariance matrix (second-order moments), of which only the latter is relevant for entanglement properties.[31] PPT criterion, which is sufficient and necessary conditions for bipartite splittings of Gaussian states with N modes with only a single mode on one side $(1|N-1)$, where N is the total number of entangled modes. The entanglement characteristic is checked by evaluating the symplectic eigenvalues of the partially transposed matrix.[32,33] In the tripartite scenario, the three possible 1×2 partitions have to be tested. All the partitions of the three mode states are inseparable when the smallest symplectic eigenvalue for each of the three partially transposed covariance matrices is smaller than 1. The smaller the symplectic eigenvalue is, the larger the entanglement becomes. Generally, the covariance matrix of the three modes can be written as

$$v = \begin{pmatrix} c_{11}^x & 0 & c_{13}^x & 0 & c_{15}^x & 0\\ 0 & c_{11}^y & 0 & c_{13}^y & 0 & c_{15}^y\\ c_{31}^x & 0 & c_{33}^x & 0 & c_{35}^x & 0\\ 0 & c_{31}^y & 0 & c_{33}^y & 0 & c_{35}^y\\ c_{51}^x & 0 & c_{53}^x & 0 & c_{55}^x & 0\\ 0 & c_{51}^y & 0 & c_{53}^y & 0 & c_{55}^y \end{pmatrix}, \tag{8}$$

where c_{pq}^x $(p,q = 1,3,5)$ represent the correlation between amplitude quadratures of output modes, c_{pq}^y is corresponding to the phase quadratures. The elements of the covariance matrix can be defined as

$$\begin{aligned} c_{pq}^x &= \frac{1}{2}\left\langle \delta\hat{X}_p^+ \delta\hat{X}_q^+ + \delta\hat{X}_q^+ \delta\hat{X}_p^+ \right\rangle,\\ c_{pq}^y &= \frac{1}{2}\left\langle \delta\hat{X}_p^- \delta\hat{X}_q^- + \delta\hat{X}_q^- \delta\hat{X}_p^- \right\rangle \end{aligned}$$

with $p,q = 1,3,5$.

After the congruence transform $v' = S^T v S$, a new matrix v' can be obtained, where S represents the symplectic trans-

formation.

$$S = I_1 \oplus \begin{pmatrix} \frac{1}{\sqrt{2}} & 0 & \frac{1}{\sqrt{2}} & 0 \\ 0 & \frac{1}{\sqrt{2}} & 0 & \frac{1}{\sqrt{2}} \\ \frac{1}{\sqrt{2}} & 0 & -\frac{1}{\sqrt{2}} & 0 \\ 0 & \frac{1}{\sqrt{2}} & 0 & -\frac{1}{\sqrt{2}} \end{pmatrix}. \quad (9)$$

Here, I_1 is an identity matrix of 2×2. The partial transposition with respect to mode k corresponds to the change of sign of the phase quadrature. The covariance matrix of a state partially transposed with respect to mode k thus reads $\nu'(T_k) = T_k \nu' T_k^T$, where T_k is a diagonal matrix with all diagonal elements equal to 1 except for $T_{2k,2k} = -1$. After block diagonalizing the partially transposed covariance matrices with respect to the mode $\hat{a}_1$, $\hat{a}_3$ and $\hat{a}_5$, we can find the corresponding smallest symplectic eigenvalues.

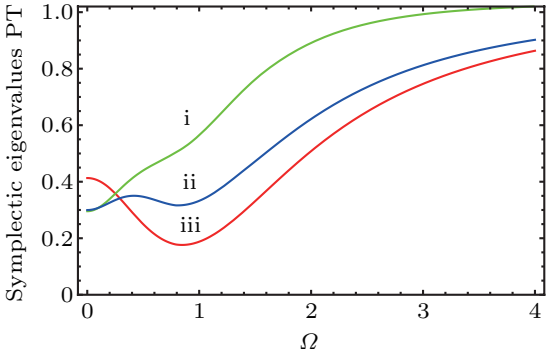

Fig. 3. (color online) The smallest symplectic eigenvalues versus normalized frequency ($\Omega = \omega/\gamma_1$) for $\gamma_1 = 0.02/\tau$, $\gamma_{b_1} = 0.018/\tau$, $\gamma_{c_1} = 0.002/\tau$, $\gamma_5 = 0.028/\tau$, $\gamma_{b_5} = 0.026/\tau$, $\gamma_{c_5} = 0.002/\tau$, $\sigma = 0.6$, $\xi = 0.7$. (i): $\hat{a}_3-(\hat{a}_1, \hat{a}_5)$, green line; (ii): $\hat{a}_5-(\hat{a}_1, \hat{a}_3)$, blue line; (iii): $\hat{a}_1-(\hat{a}_3, \hat{a}_5)$, red line.

As is shown in Fig. 3, the smallest symplectic eigenvalues of partially transposed covariance matrices with respect to the mode $\hat{a}_1$, $\hat{a}_3$ and $\hat{a}_5$ are all below 1, which means that the tripartite entanglement exists indeed in a wide frequency range, and with the increase of frequency it decreases gradually and disappears roughly at $\Omega = 4$. The maximum entanglement can be accessed at about $\Omega = 0.85$.

The smallest symplectic eigenvalues versus the pump parameter of PDC and SFG are shown in Fig. 4(a) and 4(b), respectively. It is shown that the tripartite entanglement can be obtained when $\sigma \leq 1$ and $\xi \leq 1$. The trend of the blue line $\hat{a}_5-(\hat{a}_1, \hat{a}_3)$ is different from that of the red line $\hat{a}_1-(\hat{a}_3, \hat{a}_5)$ and green line $\hat{a}_3-(\hat{a}_1, \hat{a}_5)$, because of the different origin of nonlinear process ($\hat{a}_5$ is from SFG, while $\hat{a}_1$ and $\hat{a}_3$ are from PDC).

In both Fig. 3 and Fig. 4, the red line always shows the best entanglement, which represents the entanglement between $\hat{a}_1$ and $(\hat{a}_3, \hat{a}_5)$. Because modes $\hat{a}_1$ and $\hat{a}_3$ are generated from the same PDC process, and partial quantum properties of mode $\hat{a}_3$ is transferred to mode $\hat{a}_5$ via an SFG process.

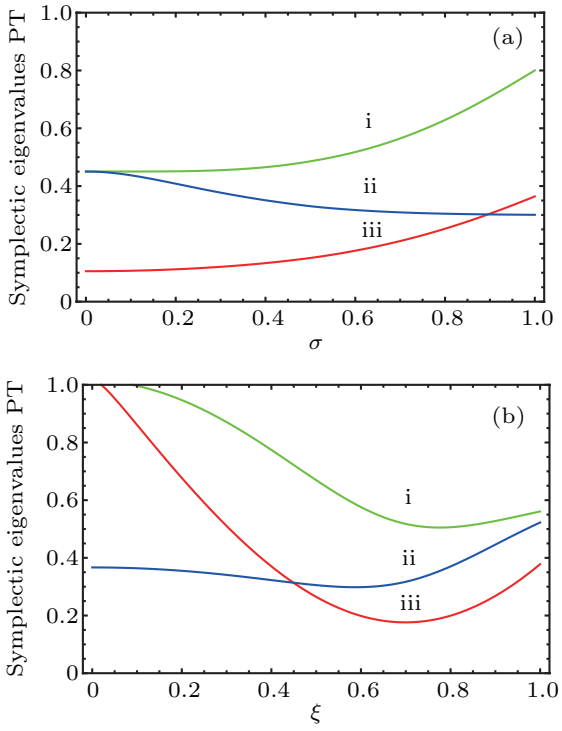

Fig. 4. (color online) The smallest symplectic eigenvalues versus pump parameters of PDC σ(a) and SFG ξ(b) for $\gamma_1 = 0.02/\tau$, $\gamma_{b_1} = 0.018/\tau$, $\gamma_{c_1} = 0.002/\tau$, $\gamma_5 = 0.028/\tau$, $\gamma_{b_5} = 0.026/\tau$, $\gamma_{c_5} = 0.002/\tau$. (a) $\sigma = \chi_1/\gamma_1$, $\Omega = 0.85$, $\xi = 0.7$; (b) $\xi = \chi_2/\gamma_1$, $\Omega = 0.85$, $\sigma = 0.6$. (i): $\hat{a}_3-(\hat{a}_1, \hat{a}_5)$, green line; (ii): $\hat{a}_5-(\hat{a}_1, \hat{a}_3)$, blue line; (iii): $\hat{a}_1-(\hat{a}_3, \hat{a}_5)$, red line.

The tripartite quantum entanglement of the 0-order and the ± 1-order comb lines are displayed in Fig. 5, and the entanglement distribution at $\pm n$-order ($n = 2, \ldots, 15$) are exactly the same, which means that each group of comb lines scaled by the same symbol in Fig. 1(b) is entangled indeed.

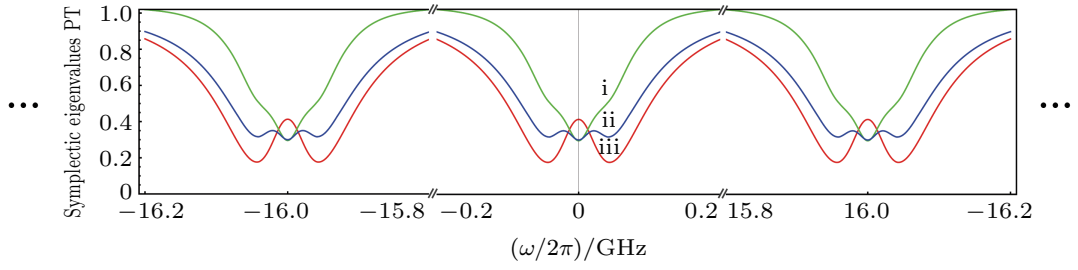

Fig. 5. (color online) The smallest symplectic eigenvalues versus analysis frequency at 0-order and ± 1-order comb lines, for $\gamma_1 = 0.02/\tau$, $\gamma_{b_1} = 0.018/\tau$, $\gamma_{c_1} = 0.002/\tau$, $\gamma_5 = 0.028/\tau$, $\gamma_{b_5} = 0.026/\tau$, $\gamma_{c_5} = 0.002/\tau$, $\sigma = 0.6$, $\xi = 0.7$. (i): $\hat{a}_3-(\hat{a}_1, \hat{a}_5)$, green line; (ii): $\hat{a}_5-(\hat{a}_1, \hat{a}_3)$, blue line; (iii): $\hat{a}_1-(\hat{a}_3, \hat{a}_5)$, red line.

Other schemes of combining frequency combs and non-classical fields have been achieved in experiment.[23,26] To realize our scheme in experiment, it should satisfy the following conditions: choosing a nonlinear crystal with proper phase-matching bandwidth, making the conversion efficiency and the strength of nonlinear interaction of each tripartite entangled states balance, designing the optical cavity with appropriate structure and cavity length. In addition, the bandwidths of mirror coating should be wide enough thus the reflection and transmission are consistent for each tripartite entangled state. Based on our theoretical scheme, the corresponding experiment setup is simple, compact and feasible.

4. Conclusion

In summary, we theoretically propose a scheme to generate 31 CV tripartite entanglement states based on optical frequency combs, in which the central wavelengths are corresponding to the optical fiber communication line and the atomic transition lines. The sufficient and necessary criterion (PPT) is used to investigate the entanglement properties of 31 tripartite modes. Based on this work, with the technology of WDM, high efficiency and high capacity can be achieved for quantum communications and quantum dense coding. We hope that such an optical device and scheme might be useful to generate valuable entanglement resources for quantum communication and quantum information storage in real quantum information networks.

References

[1] Johnson T J, Bartlett S D and Sanders B C 2002 *Phys. Rev. A* **66** 042326
[2] Jing J T, Zhang J, Yan Y, Zhao F G, Xie C D and Peng K C 2003 *Phys. Rev. Lett.* **90** 167903
[3] Madsen L S, Usenko V C, Lassen M, Filip R and Andersen U L 2012 *Nat. Commun.* **8** 1083
[4] van Loock P, Weedbrook C and Gu M 2007 *Phys. Rev. A* **76(3)** 032321
[5] Ma Y H, Yang G H, Mu Q X and Zhou L 2009 *J. Opt. Soc. Am. B* **26(4)** 713-717
[6] Nha H 2012 *Phys. Rev. A* **77** 062328
[7] van Loock P and Braunstein S L 2000 *Phys. Rev. Lett.* **84** 3482-3485
[8] Aoki T, Takei N, Yonezawa H K, Hiraoka T and Furusawa A 2003 *Phys. Rev. A* **91** 080404
[9] Su X L, Tan A H, Jia X J, Zhang J, Xie C D and Peng K C 2007 *Phys. Rev. Lett.* **98** 070502
[10] Yang R G, Wang J J, Zhang J and Sun H X 2016 *Chin, Phys .B* **25** 074208
[11] Furusawa A, Sorensen J L, Braunstein S L, Fuchs C A, Kimble H J and Polzik E S 1998 *Science* **282** 706-709
[12] Li X Y, Pan Q, Jing J T, Zhang J, Xie C D and Peng K C 2002 *Phys. Rev. Lett.* **88** 047904
[13] Allevi A, Bondani M and Paris M G A and Andreoni A 2008 *Phys. Rev. A* **78** 063801
[14] Tan A H, Xie C D and Peng K C 2012 *Phys. Rev. A* **85** 013819
[15] Yang R G, Zhai S Q, liu K, Zhang J X and Gao J R 2010 *J. Opt. Soc. Am. B* **27** 2721
[16] Li T Y, Mitazaki R, Kasai K, Okada-Shudo Y, Watanabe M and Zhang Y 2015 *Phys. Rev. A* **91** 023833
[17] Qin Z Z, Gao L M, Wang H L, Marino A M, Zhang W P and Jing J T 2014 *Phys. Rev. Lett.* **113** 023602
[18] Cai Y, Feng J L, Wang H L, Ferrini G, Xu X Y, Jing J T and Treps N 2015 *Phys. Rev. A* **91** 013843
[19] Cao L M, Qi J, Du J J and Jing J T 2017 *Phys. Rev. A* **95** 023803
[20] Wang H L, Fabre C and Jing J T 2017 *Phys. Rev. A* **95** 051802
[21] Zheng Z, Wang H L, Cheng B and Jing J T 2017 *Opt. Lett.* **42** 2754
[22] Jia X J, Yan Z H, Duan Z Y, Su X L, Wang H, Xie C D and Peng K C 2007 *Phys. Rev. Lett.* **109** 253604
[23] Pysher M, Miwa Y, Shahrokhshahi R, Bloomer R and Pfister O 2011 *Phys. Rev. Lett.* **107** 030505
[24] Yang R G, Zhang J, Zhai S Q, Liu K, Zhang J X and Gao J R 2013 *J. Opt. Soc. Am. B* **30(2)** 314-318
[25] Yang R G, Zhang J, Zhai Z H, Zhai S Q, Liu K and Gao J R 2015 *Opt. Express* **23** 21323-21333
[26] Chen M, Menicucci N C and Pfister O 2014 *Phys. Rev. Lett.* **112** 120505
[27] Pooser R and Jing J T 2014 *Phys. Rev. A* **90** 043841
[28] Yang R G, Wang J J, Zhang J, Liu K and Gao J R 2016 *J. Opt. Soc. Am. B* **33** 2424
[29] Lifshitz R, Arie A and Bahabad A 2005 *Phys. Rev. Lett.* **95** 133901
[30] Raymer M G and Noh J 2005 *Phys. Rev. A* **72** 023825
[31] Coelho A S, Barbosa F A S, Cassemiro K N, Villar A S, Martinelli M and Nussenzveig P 2009 *Science* **326** 823
[32] Simon R 2009 *Phys. Rev. Lett.* **84** 2726
[33] Vollmer C E, Schulze D, Eberle T, Handchen V, Fiurasek J and Schnabel R 2013 *Phys. Rev. Lett.* **111** 230505